

Electronic Supplementary Information

Scattering resonances in the rotational excitation of HDO by Ne and n -H₂: theory and experiment

Ricardo Manuel García-Vázquez,^a Astrid Bergeat,^{* a} Otoniel Denis-Alpizar,^b Alexandre Faure,^c Thierry Stoecklin^a and Sébastien B. Morales^a

^a Univ. Bordeaux, CNRS, ISM, 33400 Talence, France.

^b Grupo de Investigación en Física Aplicada, Instituto de Ciencias Aplicadas, Facultad de Ingeniería, Universidad Autónoma de Chile, 7500912 Santiago, Chile

^c Univ. Grenoble Alpes, CNRS, IPAG, 38000 Grenoble, France.

1 Experiments

1.1 Resonance-Enhanced Multiphoton Ionization (REMPI) and mass spectra. The HOD rotational populations of the ($X^1A_1, v = 0$) ground vibronic state were measured using (2 + 1) REMPI via the ($C^1B_1, v' = 0$) Rydbergstate¹ in the supersonic beam. Laser pulse were generated by doubling in a beta barium borate (BBO) crystal the output of a dye laser (linewidth of 0.07 cm⁻¹) operating with Coumarin 500 dye in ethanol, pumped by the third harmonic (355 nm) of a Nd:YAG laser. A small part of the visible dye laser was sent to a wavemeter to control the HDO rotational state probed, and a photodiode was monitoring the UV laser to ensure that the energy remained constant during scanning. The points associated with too small UV laser intensities were rejected to stay in the linear regime whereby the REMPI intensity only depends on the water density. The transitions, the exciting and dye-laser wavelengths used for the experimental acquisitions are reported in Table 1. The ions produced by REMPI were then probed by a two-stage time-of-flight mass spectrometer (TOF-MS), which has specially cut plates to allow the beams to pass through. A multichannel plate detector is used for ion detection. The signal is pre-amplified, gated, and integrated using a boxcar over the time-of-flight corresponding to the HDO mass, as illustrated in Fig. 1.

Table 1 Operating wavelengths used to probe the HDO rotational levels by (2+1) REMPI. The indexations, line strengths and widths are coming from pGopher² software and the spectroscopic data of Yang et al.¹

HDO($j_k a_k c_k$)	Dye laser λ / nm	Transition wavenumber / cm ⁻¹	$C^1B_1, v' = 0, j' k' a' k' c' \leftarrow X^1A_1, v = 0, j k a k c$	Relative Line Strength	Width / cm ⁻¹
0 ₀₀	495.129	80787.02	$C^1B_1, 0, 2_{21} \leftarrow X^1A_1, 0, 0_{00}$	1	4.02
0 ₀₀	495.378	80746.51	$C^1B_1, 0, 2_{11} \leftarrow X^1A_1, 0, 0_{00}$	0.16	1.53
1 ₀₁	495.222	80771.77	$C^1B_1, 0, 2_{20} \leftarrow X^1A_1, 0, 1_{01}$	1.99	4.00
1 ₁₁	495.744	80686.85	$C^1B_1, 0, 1_{10} \leftarrow X^1A_1, 0, 1_{11}$	0.90	1.53
1 ₁₀	495.774	80682.02	$C^1B_1, 0, 1_{11} \leftarrow X^1A_1, 0, 1_{10}$	0.90	1.53

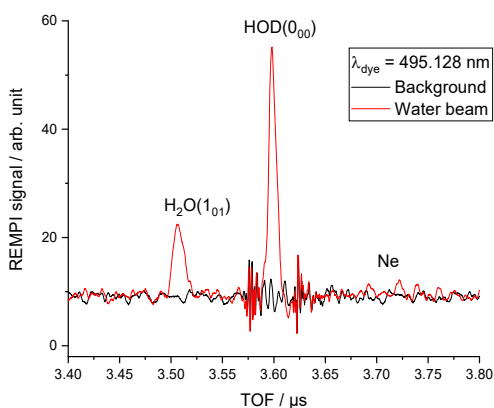


Fig. 1 Time-of-Flight Mass Spectrum of the water beam (mixture of H₂O and D₂O seeded in Ne) and the background, with an ionisation laser at 123.782 nm. The noise is due to the boxcar gate used to record the REMPI spectrum and the excitation functions.

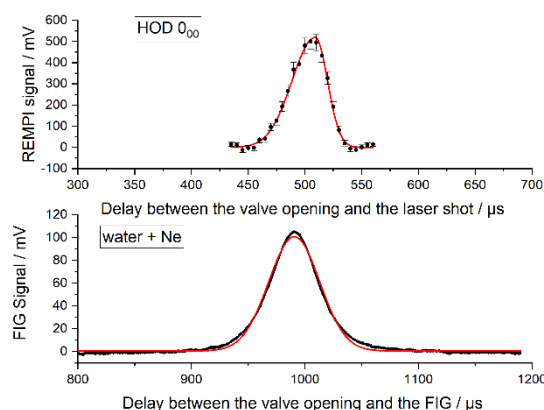


Fig. 2 Density temporal profile of HDO(0₀₀) by REMPI-MS detection at the crossing point (upper panel) and profile of Ne, the carrier gas, 393;3 nm downstream by a fast ionisation gauge.

To measure velocity distribution, pulse duration and angular spread, the density temporal profiles of HDO by REMPI-MS detection at the crossing point and of Ne, the carrier gas by a fast ionization gauge (FIG) at $d = 393.3$ mm downstream were recorded and fitted to asymmetric Gaussian profiles (Fig. 2). The details of the procedure may be found in ref.^{3, 5, 4}.

As explained in the main article, the REMPI spectrum of HDO in the water beam was fitted to determine the rotational population distribution. Mass spectra at the ionisation wavelengths given in Table 1 were also recorded, as well as the temporal density for the first excited state (Fig. 3). It should be noticed that HOD(1_{01}) density is not uniform in the water gas pulse, but these excited molecules are localised at the edges. All the mass or REMPI spectra, as well as the ICSs were recorded at the maximum of the HDO density, thus in the middle of the gas pulse. Then, the time delay between the two pulsed beams (water and the collider, Ne or H₂) was adjusted to ensure a perfect overlap of both beams at the crossing point.

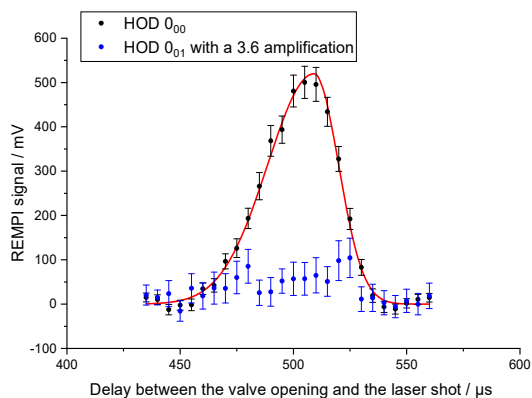


Fig. 3 Density temporal profile of HDO(0_{00} and 1) by REMPI-MS detection at the crossing point. For the first excited rotational state, an signal amplification of 3.6 by increasing the MCP voltage was applied.

1.2 HOD + Ne inelastic collisions.

REMPI spectra were recorded (Fig. 4), Ne beam being triggered at 5 Hz, with signals averaged in alternating pulse mode. Two intensities were recorded: one “background” which corresponds to HOD in the water beam and one “signal” which corresponds to HOD when the collisions between the water molecules and Ne atoms occur. This procedure was applied at two beam angles, $\theta = 15.5^\circ$ (collision energy of 21.6 cm⁻¹) and $\theta = 22.5^\circ$ (collision energy of 44.0 cm⁻¹). These two collision energies correspond to the maximum probability of HOD excitation to the 1_{01} and 1_{11} levels, respectively. It should be noticed that in the first case, the collision energy is not enough to populate the 1_{11} rotational level and the 1_{01} signal is in the noise.

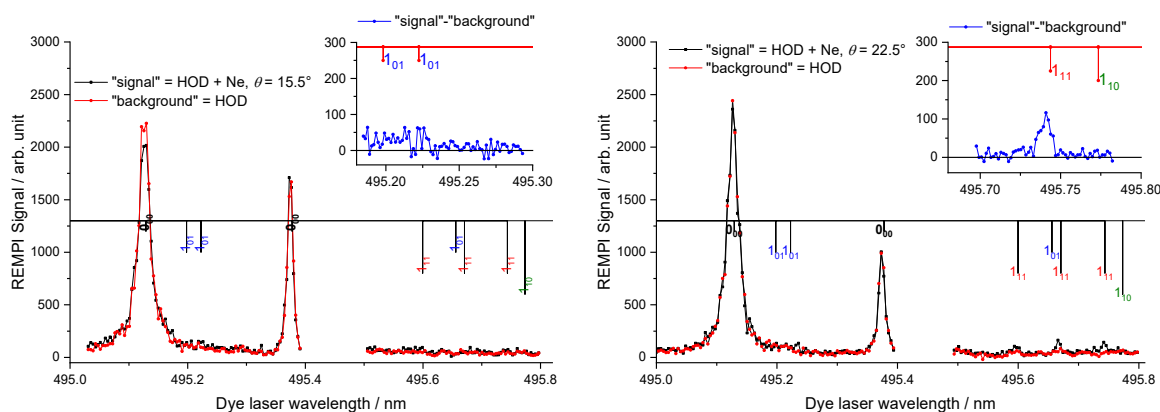


Fig. 4 (2 + 1) REMPI spectrum of the $C^1B_1, v' = 0 \leftarrow X^1A_1, v = 0$ transition of HDO in the water beam in red, when the two beams collide (Ne + water) in black (each point correspond to 30 laser shots). The difference between the “signal” and the “background” spectra were also recorded with 150 laser shots around the two transitions selected to record the excitation functions. On the left panel, the angle between the two beams was 15.5° (collision energy of 21.6 cm⁻¹) and on the right panel, 22.5° (collision energy of 44.0 cm⁻¹). The labels indicate the rotational levels $j_k a_k c_k$ from which the transition originate, for the more intense ones.

To increase the signal-to-noise ratio, mass spectra were recorded over 256 laser shots (Fig. 6).

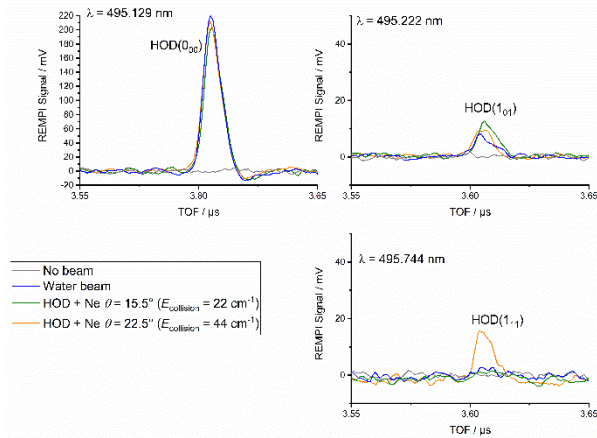


Fig. 6 Mass spectra (average of 256 laser shots) of HOD in the 0_{00} , 1_{01} and 1_{11} rotational levels. In grey, the mass spectra without any beam in the experiment (residual of HOD in the main chamber). In blue, with the water beam, only. When the two beams collide (Ne + water) with an angle of 15.5° (collision energy of 21.6 cm^{-1}) in green and 22.5° (collision energy of 44.0 cm^{-1}) in orange.

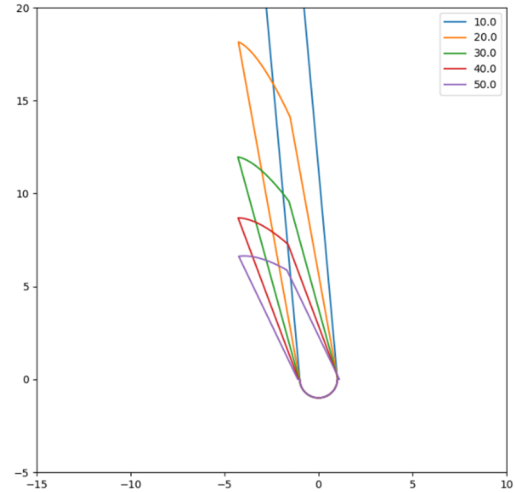


Fig. 5 The interaction volumes taken into account in the density-to-flux transformation for the angles in degree given in the figure. The water beam is vertical and the Ne beam was rotatable from 10° to 90° (90° implies an horizontal Ne beam).

The background signal from the main chamber was subtracted to the signal recorded with the water beam and also with the Ne beam at two angles (or collision energies). This intensity is then weighted with the amplification due to the voltage of the MCP. With the different experiments carried out and according to the line strengths of the corresponding REMPI transition, ratio from 1.2 to 3.8% of the 1_{01} level population to the ground 0_{00} level population was found for the water beam. Moreover, to apply the density-to-flux transformation when the two beam collide, the interaction volumes presented in Fig. 5 for different crossing angles relatively to the water beam were also taken into account (see the main article for the correction). It should be noticed that absolute cross sections couldn't be measured in our experiment because density of molecules in the molecular beam is unknown.

The rate law for the inelastic collisions between HDO and Ne of the particular probed 1_{01} rotational level density ($n_{1_{01}}$) is

$$\begin{aligned} \frac{dn_{1_{01}}}{dt} &= n_{\text{Ne}} n_{\text{HDO}} p(0_{00}) k_{0_{00} \rightarrow 1_{01}}(v_r) - n_{\text{Ne}} n_{\text{HDO}} p(1_{01}) \sum_{l=0_{00}, 1_{11}, 1_{10}, 2_{02}, 2_{12}} k_{1_{01} \rightarrow l}(v_r) \\ &= n_{\text{Ne}} n_{\text{HDO}} v_r \left(p(0_{00}) \sigma_{0_{00} \rightarrow 1_{01}}(v_r) - p(1_{01}) \sum_{l=0_{00}, 1_{11}, 1_{10}, 2_{02}, 2_{12}} \sigma_{1_{01} \rightarrow l}(v_r) \right) \end{aligned}$$

where the first term corresponds to filling up the state 1_{01} from the 0_{00} rotational level, and the second term is related to the loss of population out of this 1_{01} level. n_{Ne} is the number density of the Ne collision partner, n_{HDO} the HDO number density, and $p(0_{00}$ or $1_{01})$ the population of HDO in the rotational state 0_{00} or 1_{01} . $k_{i \rightarrow j}(v_r)$ are the rate constants at relative velocity v_r and $\sigma_{i \rightarrow j}(v_r)$ the cross-sections from the i level to the j level. The REMPI intensity is proportional to the HDO density of the 1_{01} rotational level probed. However, as we do not know the exact densities of HDO and Ne in our beams, the experimental ICSS are given in arbitrary units. To compare the experimental ICSS with the theoretical ones, we have thus added or subtracted the calculated cross-sections weighted by the appropriate initial rotational population: scenario number 1, $p(0_{00}) = 1$ and $p(1_{01}) = 0$ and scenario number 2, $p(0_{00}) = 0.95$ and $p(1_{01}) = 0.05$.

1.3 HOD + H₂ inelastic collisions.

REMPI spectra were also recorded (Fig. 8), *normal*-H₂ beam being triggered at 5 Hz, with signals averaged in alternating pulse mode. Two intensities were recorded: one "background" which corresponds to HOD in the water beam and one "signal" which corresponds to HOD when the collisions between the water molecules and *normal*-H₂ occur at a collision energy of 63 cm^{-1} . The only signal increased was the signal coming from the 1_{11} state: the difference of the two spectra "signal"- "background" is calculated and reported in the upper panel of the Fig. 8. Moreover, the analysis of the profile on the HOD(1_{01}) has again demonstrated that the water beam has some population on the first excited state mainly situated in the border of the water gas pulse, but we were not able to see any change in the signal with the collisions of H₂. These specific studies were performed at 30° and 40° , which correspond to collision energies of 29.6 and 44.6 cm^{-1} , respectively where the

calculated cross-sections present a maximum. We thus have to conclude that the cross-section should have experimentally a magnitude largely below the cross-section of the $\text{HDO} + \text{H}_2 \rightarrow \text{HDO}(1_{11}) + \text{H}_2$.

The interaction volumes taken into account in the density-to-flux transformation used for the experimental ICSs reported in the article are presented in Fig. 7 for different crossing angles relatively to the water beam.

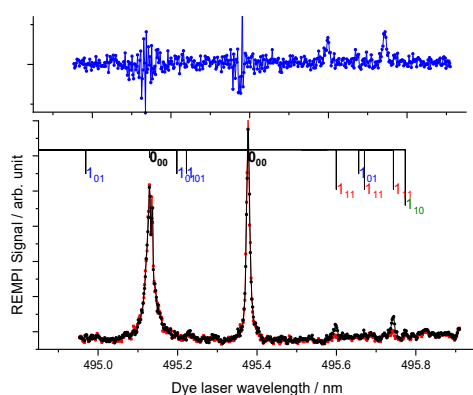


Fig. 8 $(2 + 1)$ REMPI spectrum of the $\text{C}^1\text{B}_1, v' = 0 \leftarrow \text{X}^1\text{A}_1, v = 0$ transition of HDO in the water beam in red, when the two beams collide (*normal*- H_2 + water) in black (each point correspond to 30 laser shots). In the upper panel, the difference between the two spectra of the lower panel: the signal is thus coming only from the collisions at an energy of 63 cm^{-1} . The labels indicate the rotational levels j_{kac} from which the transition originate, for the more intense ones.

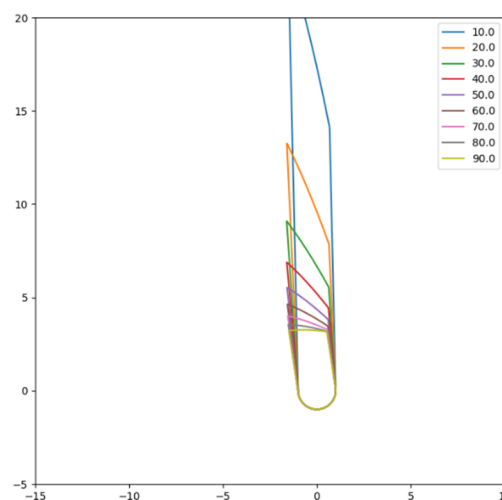


Fig. 7 The interaction volumes taken into account in the density-to-flux transformation for the angles in degree given in the figure. The water beam is vertical and the H_2 beam was rotatable from 10° to 90° (in this last case, the H_2 beam is horizontal).

- 1 C.-H. Yang, G. Sarma, J. J. ter Meulen, D. H. Parker, and C. M. Western, REMPI spectroscopy and predissociation of the $\text{C}^1\text{B}_1(v = 0)$ rotational levels of H_2O , HOD and D_2O . *Phys. Chem. Chem. Phys.*, 2010, **12**, 13983. doi:10.1039/c0cp00946f
- 2 C.M. Western. PGOPHER, A Program for Simulating Rotational, Vibrational and Electronic Spectra. *J. Quant. Spectrosc. Radiat. Trans.* 2017, **186**, 221. DOI:10.1016/j.jqsrt.2016.04.010.
- 3 A. Bergeat, S. B. Morales, C. Naulin, J. Kłos and F. Lique, *Front. Chem.*, 2019, **7**, 164. doi:10.3389/fchem.2019.00164
- 4 C. Naulin and A. Bergeat, in *Cold Chemistry: Molecular Scattering and Reactivity Near Absolute Zero*, ed. O. Dulieu and A. Osterwalder, The Royal Society of Chemistry, 2017, Chap. 3, 92. doi:10.1039/9781782626800
- 5 A. Bergeat, A. Faure, L. Wiesenfeld, C. Miossec, S. B. Morales and C. Naulin, *Molecules*, 2022, **27**, 7535. doi:10.3390/molecules27217535;